Optics Letters

Wave-band-tunable optical fiber broadband orbital angular momentum mode converter based on dispersion turning point tuning technique

Min Zhou,[1,2] Zhe Zhang,[2] Bonan Liu,[2] Shen Liu,[2] Zhiyong Bai,[2,*,†] Yu Liu,[1,3,†] Yu Pang,[1] and Yiping Wang[2]

[1]The School of Communication and Information Engineering, Chongqing University of Posts and Telecommunications, Chongqing, 400065, China
[2]Key Laboratory of Optoelectronic Devices and Systems of Ministry of Education/Guangdong Province, College of Physics and Optoelectronic Engineering, Shenzhen University, Shenzhen 518060, China
[3]e-mail: liuyu@cqupt.edu.cn
*Corresponding author: baizhiyong@szu.edu.cn
†These authors contributed equally to this work.

Received 28 July 2022; revised 1 September 2022; accepted 26 September 2022; posted 30 September 2022; published 26 October 2022

A wave-band-tunable optical fiber broadband orbital angular momentum (OAM) mode converter based on a helical long-period fiber grating (HLPFG) and dispersion turning point (DTP) tuning technique is demonstrated both theoretically and experimentally. The DTP tuning is achieved by thinning the optical fiber during the HLPFG inscription. As a proof of concept, the DTP wavelength of the $LP_{1,5}$ mode is successfully tuned from the original ~2.4 μm to ~2.0 μm and ~1.7 μm. With the help of the HLPFG, broadband OAM mode conversion ($LP_{0,1}$→$LP_{1,5}$) is demonstrated near the 2.0 μm and 1.7 μm wave bands. This work addresses a long-standing problem that the broadband mode conversion is limited by the intrinsic DTP wavelength of the modes and provides a new, to the best of our knowledge, alternative for broadband OAM mode conversion at the desired wave bands.

https://doi.org/10.1364/OL.471904

An all-fiber orbital angular momentum (OAM) mode converter is a key device to improve the transmission capacity of an optical fiber communication system since the OAM mode can carry rich information in a new dimension. Meanwhile, the bandwidth of the OAM mode converter is another important parameter since the bandwidth is proportional to the capacity in wavelength-division multiplexing (WDM) and mode-division multiplexing (MDM) optical fiber telecommunication systems [1–4]. Various all-fiber OAM mode converters based on optical fiber couplers [5,6], long-period fiber gratings (LPFGs) [7–11], and helical long-period fiber gratings (HLPFGs) [12–17] have been demonstrated in the last decade. The most popular among them is HLPFGs, which not only have high mode conversion efficiency and low insertion loss, but are polarization insensitive. In recent years, much attention has been paid on expanding the bandwidth of the HLPFG-based OAM mode converter. The strategies mainly include cascading two HLPFGs [18,19] and using phase shifted HLPFGs [20,21]. However, the achieved bandwidth for a cascaded HLPFG is only a few tens of nanometers. In 2021, Zhu *et al*. numerically demonstrated an ultra-broadband OAM mode converter with a bandwidth of ~469 nm by using a phase shifted HLPFG [21]. However, experimental demonstration is too difficult, and hence has not been reported yet.

Dispersion turning point (DTP) of the fiber modes can be employed to achieve broadband mode conversion, which was first proposed and demonstrated by Shu *et al.* in 1999 [22]. Based on this principle, broadband OAM mode conversion can be achieved by designing HLPFG parameters according to the DTP wavelength [23–28]. In 2020, Zhao *et al*. demonstrated a broadband mode converter based on an HLPFG operating at a wavelength near the DTP, and a bandwidth of 297 nm @ −10 dB was achieved [25]. In 2020, Ren *et al*. numerically demonstrated the feasibility of a dual-resonant HLPFG in a conventional single-mode fiber (SMF) for broadband OAM generation, where the obtained bandwidth was 287 nm @ −3 dB [26]. However, the DTP wave band for a determined mode for a fiber is fixed, meaning that broadband OAM mode conversion is limited to a determined wave band (i.e., the DTP wave band of the modes).

In this paper, we propose a DTP tuning technique during the HLPFG inscription. As a proof of concept, the DTP wavelength of the $LP_{1,5}$ mode of a conventional SMF is successfully tuned from the original ~2.4 μm to ~2.0 μm and ~1.7 μm, confirming our theoretical calculations and predictions. With the help of the HLPFG, broadband OAM mode conversion ($LP_{0,1}$→$LP_{1,5}$) near 2.0 μm and 1.7 μm is demonstrated. This work addresses a long-standing problem that broadband mode conversion is limited by the intrinsic DTP wavelength and provides a new alternative for broadband OAM mode conversion.

An HLPFG is typically formed by periodic helical refractive index modulation along the longitudinal axis of an optical fiber. With the help of the HLPFG, the fundamental core mode of a conventional SMF can be effectively converted into the high-order cladding modes with helical phase without the need for polarization control, as shown in Fig. 1. The excitation of the

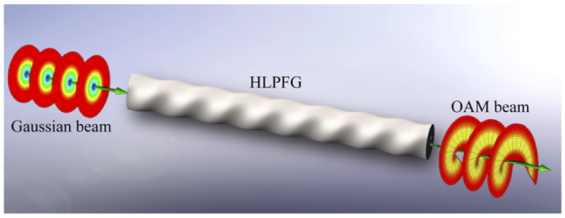

Fig. 1. Schematic diagram of all-fiber OAM mode conversion using a helical long-period fiber grating.

OAM mode by the HLPFG needs not only phase matching of the modes but angular momentum conservation [13,29]:

$$m \cdot \lambda = (n_F - n_N) \cdot \Lambda, \tag{1}$$

$$m \cdot \sigma = J_N - J_F, \tag{2}$$

where m is the order of the harmonic term, which determines the topological charge number of the OAM mode. Here, n_F, n_N and J_F, J_N are the effective refractive index (RI) and total angular momentum of the fundamental core mode and high-order cladding mode, respectively; λ and Λ represent the resonant wavelength and grating period, respectively; σ represents the helicity of the HLPFG; and σ values with 1 and −1 represent the left- and right-handed HLPFG, respectively. As such, an HLPFG is a convenient device for all-fiber OAM mode conversion without the demand for complex polarization control.

The conversion bandwidth of the OAM mode is another vital concern. However, the most popular schema that uses the DTP of the mode suffers difficulties since the DTP wavelength of a determined mode is a constant, meaning that broadband OAM conversion for a determined mode is merely achievable at a determined wave band (near the intrinsic DTP wavelength). Using conventional SMF parameters (core diameter, dco =8.4 μm; cladding diameter, dcl =125 μm; and the RI difference, 0.0054), we calculate the dispersion curve and resonant wavelength of

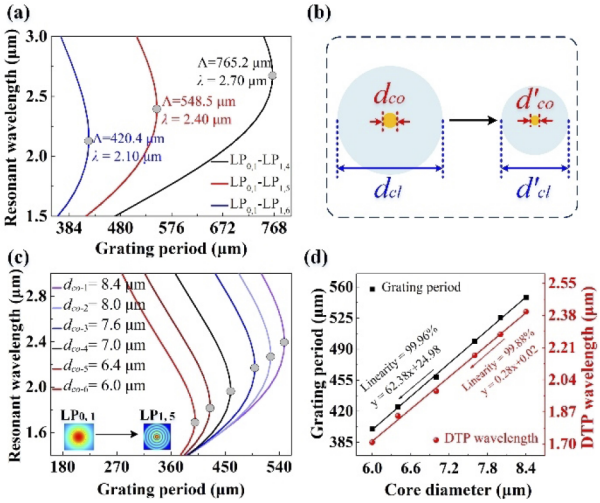

Fig. 2. (a) Calculated resonant wavelength of the three cladding modes ($LP_{1,4}$, $LP_{1,5}$, and $LP_{1,6}$) of a conventional SMF versus grating period. (b) Sketch of optical fiber thinning. (c) Calculated resonant wavelength of the $LP_{1,5}$ mode versus grating period for different fiber diameters. (d) DTP wavelength of $LP_{1,5}$ mode (red dots) and the need grating period (black bars) for $LP_{0,1} \rightarrow LP_{1,5}$ mode conversion versus the core diameters.

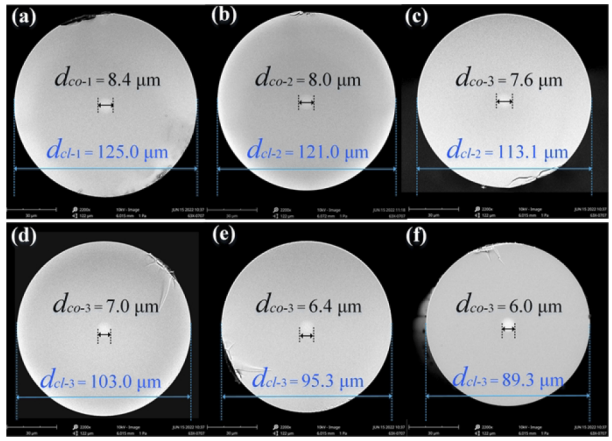

Fig. 3. Scanning electronic microscopy (SEM) images of the fiber cross sections.

an HLPFG for different cladding modes ($LP_{1,4}$, $LP_{1,5}$, and $LP_{1,6}$) versus grating period Λ, as shown in Fig. 2(a). The intrinsic DTP wavelength of the $LP_{1,5}$ mode is ~2.4 μm, corresponding a grating period of 548.5 μm [the red curve in Fig. 2(a)].

Can the dispersion curve and DTP wavelength be changed when thinning the optical fiber [as shown in Fig. 2(b)]? We calculate the dispersion curves and the corresponding resonant wavelength of the $LP_{1,5}$ mode for a thinned optical fiber with different core diameters, as shown in Fig. 2(c). The DTP wavelengths for the $LP_{1,5}$ mode are ~2.40 μm, ~2.28 μm, ~2.17 μm, ~1.98 μm, ~1.85 μm, and ~1.71 μm for the fibers with core diameters of ~8.40 μm, ~8.00 μm, ~7.60 μm, ~7.00 μm, ~6.40 μm, and ~6.00 μm, respectively. The corresponding grating periods for $LP_{0,1}$ mode to $LP_{1,5}$ mode conversion are ~525.7 μm, ~499.2 μm, ~458.7 μm, ~424.9 μm, and ~400.0 μm, respectively. The DTP wavelength and the grating period versus the fiber core diameters are shown in Fig. 2(d), where a nearly linear relationship is observed ($R^2 > 99\%$). In the calculations, the ratio of the core diameter to cladding diameter is assumed to be unchanged. The simulation results provide us with a promising way to tune the DTP wavelength of a determined fiber mode. In combination with an HLPFG, a broadband OAM mode converter with wave band tunability is available.

In the experiment, a fiber axial tapering function is added to our homemade oxyhydrogen-flame HLPFG inscription setup that has been detailed in our previous work [27,30]. By the improved setup, optical fiber thinning can be flexibly controlled during the HLPFG inscription process. Six HLPFGs are inscribed in the thinned optical fibers that have core diameters of ~8.40 μm, ~8.00 μm, ~7.60 μm, ~7.00 μm, ~6.40 μm, and ~6.00 μm and the scanning electron microscopy (SEM) images of the fiber cross section are taken and presented in Figs. 3(a)–3(f), respectively.

According to the simulations in Fig. 2, the DTP wavelength of the $LP_{1,5}$ mode can be tuned to a shorter wavelength (~1.98 μm and ~1.71 μm for fiber diameters of ~7.0 μm and ~6.0 μm, respectively) by thinning the optical fiber. We first measure the transmission spectra of two thinned HLPFGs that have the same core diameters of ~7.0 μm but with a grating period of 452.8 μm and 450.7 μm, respectively. Resonances can be clearly observed in the transmission spectra, as shown in Fig. 4. The −10-dB bandwidths of the resonances are measured to be ~217 nm and ~324 nm, respectively. The central wavelength of the resonance

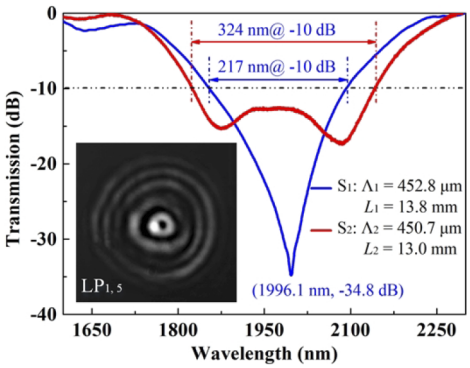

Fig. 4. Transmission spectra of the two HLPFGs with the same core diameters of ~7.0 μm but with grating periods of ~452.8 μm (blue curve) and ~450.7 μm (red curve). Inset shows the mode field profile of one of the HLPFGs measured at 1.989 μm.

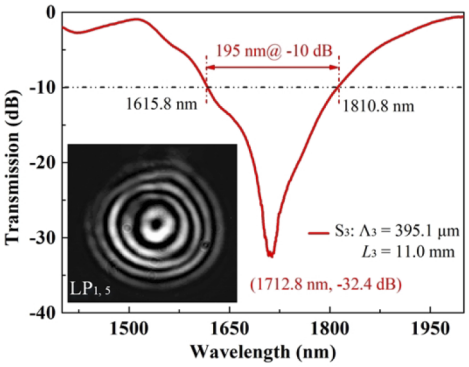

Fig. 5. Transmission spectrum of the HLPFG with a fiber core diameter of ~6.0 μm and grating period of ~395.1 μm. Inset shows the mode field profile of the HLPFG measured at ~1.989 μm.

is ~1.996 μm, which is a slight deviation from the simulation result (1.98 μm). The slight deviation may be attributed to the measurement errors of the fiber diameters.

To verify the mode order of the resonance and because of the lack of narrow-bandwidth source at this wave band, we develop a light source with a center wavelength of ~1.989 μm and a full width at half maximum (FWHM) of 1.32 nm by fusion splicing a fiber Bragg grating filter to a supercontinuum light source (YSL-SC-5-FC) in a reflective working manner. The mode field image is taken and shown in the inset of Fig. 4, where the $LP_{1,5}$ mode is clearly identified. The method for mode field characterization is similar to our previous works [31,32].

We further explore the wave band tunability of the DTP of the $LP_{1,5}$ mode by thinning the optical fiber further during HLPFG inscription. The core diameter is reduced to ~6.0 μm and the grating period is set as ~395.1 μm. The transmission spectrum of the HLPFG is measured and shown in Fig. 5, where the resonance centered at ~1712.8 nm with a −10-dB bandwidth of ~195 nm is identified. We measure the mode field distribution of the resonance using a wavelength-tunable laser source (KEYSIGHT-N7776C, 1450–1650 nm) at 1650 nm to verify the order of the resonant mode. Just like the theoretical calculations, the $LP_{1,5}$ mode is clearly observed, as shown in the inset of Fig. 5.

The phase properties of the excited $LP_{1,5}$ mode is further characterized by a conventional interferometric approach [10,27]. The mode field distributions of the excited $LP_{1,5}$ mode at

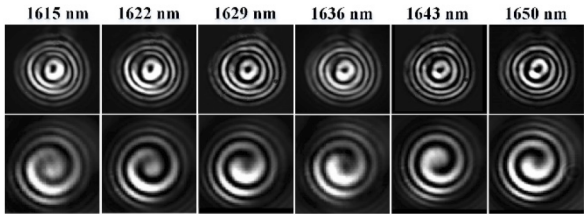

Fig. 6. (Top row) Measured mode field distributions of the HLPFG (S_3) and (bottom row) its interference patterns with Gaussian beams within the wavelength range of 1615–1650 nm.

wavelengths of ~1615 nm, ~1622 nm, ~1629 nm, ~1636 nm, ~1643 nm, and ~1650 nm are measured and shown in the top row of Fig. 6 and the corresponding interference patterns are shown in the bottom row. The counterclockwise vortex patterns imply OAM modes with a topological charge number of +1. As such, broadband OAM mode conversion ($LP_{0,1}$ to $LP_{1,5}$) at a tunable wave band (from ~2.4 μm to ~2.0 and ~1.7 μm) is experimentally demonstrated.

In conclusion, we demonstrate a wave-band-tunable optical fiber broadband OAM mode converter using our developed DTP tuning technique during the HLPFG inscription. The DTP wavelength of the $LP_{1,5}$ mode of a conventional SMF is successfully tuned from ~2.4 μm to ~2.0 μm and ~1.7 μm, and with the help of HLPFGs, broadband OAM mode conversion ($LP_{0,1}\rightarrow LP_{1,5}$) is demonstrated at the ~2.0 μm and ~1.7 μm wave bands. This work provides a new approach for DTP wavelength tuning of the fiber modes and thus enables the broadband OAM mode conversion at a larger dynamic wavelength range. The proposed schema may be widely appliable for broadband OAM mode conversion in few-mode fiber systems.

Funding. Shenzhen Science and Technology Program (RCBS202007141 14922296); National Natural Science Foundation of China (52175531, 61875134); Basic and Applied Basic Research Foundation of Guangdong Province (32221295).

Disclosures. The authors declare no conflicts of interest.

Data availability. Data underlying the results presented in this paper are not publicly available at this time but may be obtained from the authors upon reasonable request.

REFERENCES

1. J. Wang, J. Yang, I. M. Fazal, N. Ahmed, Y. Yan, H. Huang, Y. Ren, Y. Yue, S. Dolinar, M. Tur, and A. E. Willner, Nat. Photonics **6**, 488 (2012).
2. N. Bozinovic, Y. Yue, Y. Ren, M. Tur, P. Kristensen, H. Huang, A. E. Willner, and S. Ramachandran, Science **340**, 1545 (2013).
3. W. Huang, Y. You, B. B. Song, and S. Y. Chen, Optoelectron. Lett. **16**, 34 (2020).
4. A. Rjeb, H. Fathallah, S. Chebaane, and M. Machhout, Optoelectron. Lett. **17**, 501 (2021).
5. T. Wang, F. Wang, F. Shi, F. F. Pang, S. j. Huang, T. Y. Wang, and X. L. Zeng, J. Lightwave Technol. **35**, 2161 (2017).
6. F. Xia, Y. Zhao, H. F. Hu, and Y. Zhang, Opt. Laser Technol. **112**, 436 (2019).
7. H. Wu, S. C. Gao, B. S. Huang, Y. H. Feng, X. C. Huang, W. P. Liu, and Z. H. Li, Opt. Lett. **42**, 5210 (2017).
8. X. C. Huang, S. S. Xiong, J. G. Chen, S. C. Gao, R. L. Xiao, Y. H. Feng, and W. P. Liu, Infrared Phys. Technol. **116**, 103760 (2021).
9. M. Feng, W. Z. Chang, B. W. Mao, H. Y. Guo, Z. Wang, and Y. G. Liu, Opt. Laser Technol. **152**, 108131 (2022).

10. Z. Y. Bai, M. Q. Li, Y. P. Wang, J. Tang, Z. Zhang, S. Liu, C. L. Fu, Y. Zhang, J. He, Y. Wang, and C. R. Liao, Appl. Phys. Express **12**, 072004 (2019).
11. M. Deng, J. S. Xu, Z. Zhang, Z. Y. Bai, S. Liu, Y. Wang, and Y. P. Wang, Opt. Express **25**, 14308 (2017).
12. J. Y. Chen, Z. Y. Bai, G. X. Zhu, R. Liu, C. R. Huang, Z. Huang, L. P. Wu, C. R. Liao, and Y. P. Wang, Opt. Express **30**, 4402 (2022).
13. H. Zhao, P. Wang, T. Yamakawa, and H. P. Li, Opt. Lett. **44**, 5370 (2019).
14. M. Zhou, Z. Zhang, T. Zou, L. P. Shao, S. Liu, Z. Y. Bai, Y. Pang, Y. Liu, and Y. P. Wang, Opt. Lett. **47**, 3896 (2022).
15. Z. Bai, Y. Wang, Y. Zhang, C. Fu, and J. He, IEEE Photonics Technol. Lett. **32**, 418 (2020).
16. T. S. Detani, H. Zhao, P. Wang, T. G. Suzuki, and H. P. Li, Opt. Lett. **46**, 949 (2021).
17. Z. Huang, Z. Y. Bai, G. X. Zhu, C. R. Huang, J. Y. Chen, S. Liu, C. L. Fu, J. He, and Y. P. Wang, Opt. Express **29**, 39384 (2021).
18. P. Wang, H. Zhao, T. Detani, and H. P. Li, IEEE Photonics Technol. Lett. **32**, 685 (2020).
19. C. L. Fu, P. F. li, Z. Y. Bai, S. Liu, and Y. P. Wang, Opt. Lett. **45**, 5032 (2020).
20. P. Wang, H. Zhao, T. Yamakawa, and H. Li, IEEE Photonics Technol. Lett. **32**, 170 (2020).
21. C. Zhu, L. Wang, Z. Bing, R. Tong, M. Chen, S. Hu, Y. Zhao, and H. Li, IEEE J. Quantum Electron. **57**, 1 (2021).
22. X. W. Shu, X. Zhu, Q. Wang, S. Jiang, W. Shi, Z. Huang, and D. Huang, Electron. Lett. **35**, 649 (1999).
23. J. Li, J. T. Liu, H. F. Hu, Y. Zhao, and F. Xia, IEEE Photonics Technol. Lett. **29**, 2103 (2017).
24. Y. Guo, Y. G. Liu, Z. Wang, H. Zhang, and Z. Li, Opt. Laser Technol. **118**, 8 (2019).
25. X. Zhao, Y. Liu, Z. Liu, and C. Mou, Opt. Express **28**, 11990 (2020).
26. K. L. Ren, M. H. Cheng, L. Y. Ren, Y. H. Jiang, D. D. Han, Y. K. Wang, J. Dong, J. H. Liu, L. Yang, and Z. Q. Xi, OSA Continuum **3**, 77 (2020).
27. M. Zhou, Z. Zhang, L. P. Shao, S. Liu, Y. Liu, Y. Pang, Z. Y. Bai, C. L. Fu, W. Cui, L. Qi, and Y. P. Wang, Opt. Express **29**, 15595 (2021).
28. H. Zhao, Z. Zhang, M. M. Zhang, Y. Y. Hao, P. Wang, and H. P. Li, Opt. Express **29**, 29518 (2021).
29. M. Napiorkowski and W. Urbanczyk, Opt. Lett. **43**, 395 (2018).
30. S. Liu, M. Zhou, L. P. Shao, Z. Zhang, Z. Y. Bai, and Y. P. Wang, Opt. Express **30**, 21085 (2022).
31. Z. Zhang, W. Ding, A. Q. Jia, Y. F. Hong, Y. Chen, Y. Z. Sun, and Y. Y. Wang, Opt. Express **30**, 15149 (2022).
32. Z. Zhang, Y. F. Hong, Y. L. Sheng, A. Q. Jia, X. Q. Liu, S. F. Gao, W. Ding, and Y. Y. Wang, Opt. Lett. **47**, 3199 (2022).